

We are IntechOpen, the world's leading publisher of Open Access books Built by scientists, for scientists

6,900

Open access books available

185,000

International authors and editors

200M

Downloads

Our authors are among the

154

Countries delivered to

TOP 1%

most cited scientists

12.2%

Contributors from top 500 universities



WEB OF SCIENCE™

Selection of our books indexed in the Book Citation Index
in Web of Science™ Core Collection (BKCI)

Interested in publishing with us?
Contact book.department@intechopen.com

Numbers displayed above are based on latest data collected.
For more information visit www.intechopen.com



DLC Coating on Magnesium Alloy Sheet by Low-Temperature Plasma for Better Formability

Yu IRIYAMA and Shoichiro YOSHIHARA
*University of Yamanashi
 Japan*

1. Introduction

Magnesium (Mg) alloy has been attracting great attention as a promising light-metal material which has various potential applications because of its various unique and great properties. They are, for example, a smaller density, about two-thirds of Al, the greatest specific strength among all the metals, superior machining property, shielding of electromagnetic wave, and vibration absorbability. Taking advantage of them, Mg is expected to be used as structural components for automobile, lap-top computer, cell phone, and you name it, and it could replace aluminum in many areas. In general, the weight of any products with Mg body would be reduced which enables us to handle the products easier. More specifically, for example, Mg body could increase the gas mileage of automobile and protect computers and cell phones from unexpected vibration or electromagnetic waves.

In spite of the numerous advantages, however, Mg materials have not been used widely up to now. It is because there is a drawback to the workability in Mg. In the metal forming process, in general, press forming is popular, which increases the productivity and decreases the manufacturing cost and environmental load. However, since seizing of Mg in press forming is easily happened, forming of Mg is often processed by forging and die-casting. The formability of Mg alloys is especially poor at room temperature because of their hexagonal close-packed structure. Hence, there are few slip planes in the case of a pyramid surface or cylinder surface at room temperature. Furthermore, these slip planes are easily activated at elevated temperatures. Therefore, the deep-drawing process of Mg alloy sheets is generally conducted at high temperatures (approximately 200 °C). During the deep-drawing process, even at an elevated temperature, it is necessary to use a lubricant, such as molybdenum disulfide (MoS₂) based grease, which can maintain the performance. However, such lubricants have disadvantages such as a high cost, difficulty in degreasing and poor workability. Moreover, the large amount of lubricant waste raises has an adverse effect on the environment. Therefore, new techniques of lubrication that have less impact on the environment are immediately required.

In recent years, various studies on dry press forming, which does not involve the use of any lubricants during plastic processing, have been performed (Kataoka, 2006).

Dry press forming is also attractive as a forming technique with zero emissions. However, it is difficult to apply this method to the forming of metal sheets.

The feasibility of deep-drawing has been studied using ceramic dies (Kataoka et al., 2004). Ceramic dies have been successfully applied to the deep drawing of mild steel and pure copper sheets but not to the deep-drawing of titanium sheets. In the deep-drawing of metal alloy sheets, a pretreatment, in which an adhesive tribological coating is formed, is effective for improving workability when using alumina and zirconia dies. Adapting the design of the ceramic die to each material is indispensable for realizing dry forming. However, the workability of ceramic tools is poor for complicated shapes, which is limited to simple shapes. Thus, the use of electroconductive ceramic tools has been proposed (Tamaoki et al., 2006). Electroconductive ceramic tools can be formed by electrical discharge machining methods. Using an electroconductive ceramic as a plastic-forming tool, high drawability was confirmed and the dry deep-drawing of what was successfully performed up to 10,000 times.

We have also tried to increase formability of Mg alloy sheet, and obtained some good results by local heating-cooling technique (Yoshihara et al., 2003) and the control of blank holder force (Yoshihara et al., 2005) in deep-drawing process.

Diamond-like carbon (DLC) thin film could be a promising alternative to the wet lubricant. DLC is a general term of amorphous carbon or hydrocarbon, expressed as a-C or a-C:H, which is stable in chemically and physically and has a low friction coefficient. DLC is usually prepared by plasma CVD using hydrocarbon monomer gases such as methane. This dry process has been reevaluated as an environmentally friendly system in recent years since it exhausts little hazardous and toxic compounds and it does not require drying process, which can save energy and time. Similarly, DLC coating is not a new technique, but it has been regaining more expectation recently and many applications have been proposed. DLC coating on Mg is one of them, of which research have been reported on not only lubrication but also corrosion protection (Yamauchi et al., 2005; Konca et al., 2006; Yamauchi et al., 2007; Choi et al., 2007a; Choi et al., 2007b; Wu et al., 2010; Dai et al., 2010).

The use of a die coated with DLC for deep-drawing has been proposed owing to the excellent tribological properties of DLC (Kataoka et al., 2005). The use of a DLC coating has been found to eliminate the need for any lubricants to prevent the adhesion of aluminum to the die material. Also, the DLC coating prolongs the die lifetime to up to 10,000 deep-drawing operations.

Similarly, the use of a die coated with a chemical vapor deposition (CVD) diamond film has also been proposed, because the film has superior tribological properties to a DLC film (Tamaoki et al., 2007). It was confirmed that CVD-diamond-coated dies could perform for 100,000 deep-drawing operations on a stainless-steel sheet (SUS304) without the use of lubricants.

On the other hand, a thin hard film coating such as a DLC coated can also be used to improve the lifetime and dimensional accuracy of tools (D'Errico et al., 1998). For instance, thin PVD layers can be coated on a mold to increase the lifetime of tools (Reisal et al., 2003; Tillmann et al., 2009).

The surface of tools is easily damaged upon coming into contact with hard materials and by repeated scratching. For the prolongation of the tool lifetime, thin layers deposited by PVD have been employed. It was confirmed that the tool lifetime was increased when the friction between the tool and hard materials was reduced by the PVD layer. Many studies of coating technique for tools in press forming have been practiced.

In our research, we coated DLC film on Mg alloy sheet using low-temperature plasma in order to reduce the surface friction, which enables the Mg alloy sheet to be press-formable without lubricant. We mainly introduce and present our original experimental results on

this subject. And in the last section, we added some data of DLC coated Al alloy sheet. The formability of Al is superior to Mg, but it still requires lubricant even at an elevated temperature.

2. Nomenclature

- BHF
- : Blank holder force
- CVD
- : Chemical vapor deposition
- D
- : Blank diameter
- D_d
- : Die diameter
- D_p
- : Punch diameter
- DLC
- : Diamond-like carbon
- $DR = (D/D_p)$
- : Drawing ratio
- $LDR = (D_{max}/D_p)$
- : Limiting drawing ratio
- R_p
- : Punch shoulder radius
- R_d
- : Die shoulder radius
- RF
- : Radio frequency
- R_a
- : Average of surface roughness
- R_z
- : Maximum height of surface roughness
- RD
- : Rolling direction
- TD
- : Transverse direction
- TEOS
- : Tetraethoxysilane

3. Experimental procedure and evaluation methods

3.1 Materials

Used Mg alloy sheet was 0.5-mm thick AZ31B-O, which was purchased from Osaka Fuji Corp. The composition of AZ31B-O is listed in Table 1. As shown in this table, the Mg alloy contains about 3% of Al, 1% of Zn, and small amounts of Mn and Si. The Mg alloy sheet was cut into suitable sizes for each testing and characterizing method, and cleaned ultrasonically in distilled ethanol before use.

Al	3.5	Ca	<0.01
Zn	0.9	Ni	<0.001
Mn	0.64	Fe	0.002
Si	0.01	Mg	balance
Cu	<0.01		

Table 1. Composition (%) of Mg alloy sheet, AZ31B-O

As gases for plasma CVD of DLC, methane and hydrogen were used. As for plasma deposition of silicon layer, tetraethoxysilane ($\text{Si}(\text{OC}_2\text{H}_5)_4$) was used. As lubricants for deep drawing, MoS_2 and GM100 (Nihon Kohsakuyu Co., $\nu = 38.38 \text{ mm}^2/\text{s}$ at 40°C) were used.

3.2 DLC coating

DLC coating and silicon-layer coating were carried out with a plasma polymerization apparatus (Samco International, PD-S10) shown in Figure 1. Most of the cases, silicon layer was coated first on Mg alloy sheet, then DLC was coated continuously without breaking the vacuum. A capacitively coupled radio-frequency (13.56 MHz) plasma was created between a pair of stainless-steel electrodes (160-mm d., 60-mm gap). Mg alloy sheet samples were placed underneath of the top electrode, to which the power was supplied. The electrode was not heated intentionally. The flow rate of TEOS was controlled with a needle valve while methane and hydrogen were introduced into the reactor through a mass flow controller (Tylan FC-770A). The pressure of the system was monitored with an absolute pressure gauge (MKS Baratron 122AA). During the plasma coating, deposition rate and total thickness were monitored with a deposition monitor (Leybold Inficon, XTM/2) that had a quartz oscillator sensor coated with gold, which was placed beside the bottom and ground electrode.

The deposition was conducted at the plasma power of 150 W and various flow rates and durations. The standard plasma condition for TEOS coating was 150 W, 3 sccm, 3 min, and that for DLC coating was 150 W, 10 min, 25 sccm of the mixture of CH₄ and H₂.

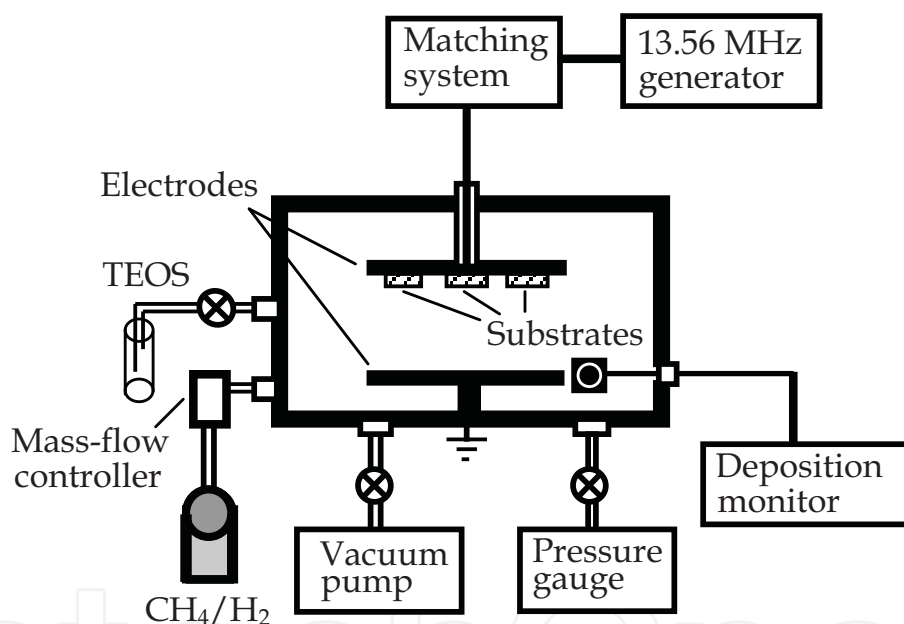


Fig. 1. Low-temperature plasma reactor used for DLC and silicon layer coatings (Iriyama et al., 2008)

3.3 Surface analysis

In addition to the thickness measurement with a deposition monitor placed beside the bottom electrode, we measured the thickness directly on the sample with a surface profile measuring system (ULVAC, Dektak3 ST).

Surface chemical composition of DLC coated Mg alloy sheets were analyzed with X-ray photoelectron spectroscopy (XPS, JEOL, JPS-9200).

In compensation for the data of XPS, glow discharge spectroscopy (GDS, Rigaku GDA750) was used for the analysis of surface concentration of hydrogen.

Surfaces of DLC coated Mg alloy sheets were observed with scanning electron microscope (SEM, Elionix, EXM-3500).

The surface roughness was measured in the direction of the TD cross section. The sliding speed was 0.1 mm/s, the sliding distance was 3-5 mm and surface roughness was measured at regular intervals of 0.002 mm. The reference length was 0.8 mm.

3.4 Adhesion test

For the evaluation of the adhesivity of the DLC coatings on Mg alloy sheet, cross-cut test was carried out. In the test, the surface layer of DLC coated Mg alloy sheet was cut straight with 1-mm interval for X- and Y-axes to make one-hundred 1-mm squares in a 10-mm square. An adhesive tape (Nichiban, Serotepu) was placed on it with a good contact. Then the tape was pulled back toward 180° angle. The adhesivity was evaluated from the number of unpeeled squares out of 100.

3.5 Friction test

Friction tests were carried out using a ball-on-disc type friction-testing machine (tribometer). Figure 2 shows a schematic illustration of the friction testing machine and Table 2 shows the conditions of the friction tests. The 0.5 N of vertical load was applied to Mg alloy sheet (30-mm d.) on the turntable. The friction coefficient was measured while the turntable was rotated at a circumferential velocity of 10 mm/s.

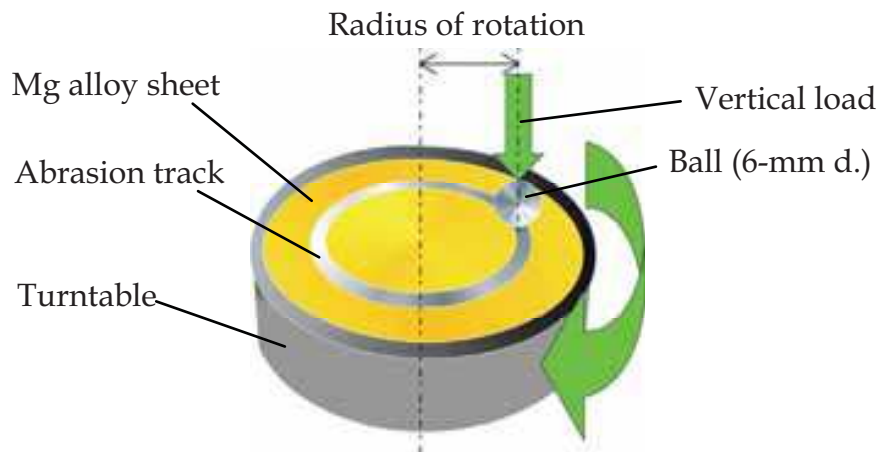


Fig. 2. Schematic illustration of friction test machine (Tsuji et al., 2009)

Vertical load (N)	0.5
Circumferential velocity (mm/s)	10
Rotation frequency (rpm)	30
Radius of rotation (mm)	10
Ball material	SUJ2

Table 2. Experimental condition of friction test (Tsuji et al., 2009)

3.6 Circular-cup deep-drawing test

Figure 3 is a schematic illustration of the deep-drawing apparatus and Table 3 shows typical conditions in the deep-drawing test. The compact press-forming machine with the capability of providing a punch thrust force of 5 kN was used in this experiment. This machine can generate an arbitrary blank-holding force and punch speed.

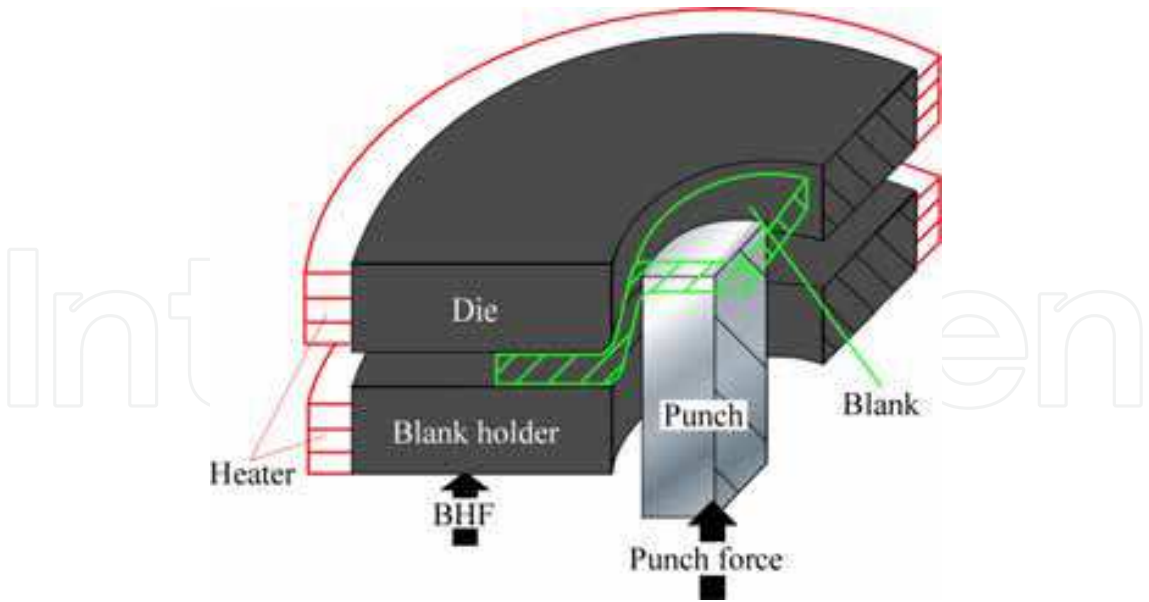


Fig. 3. Schematic illustration of deep-drawing equipment (Tsuji et al., 2009)

Punch speed (mm/s)		0.5
BHF (N)		50, 100, 150, 200, 250, 300
Temperature (°C)		200
Drawing ratio ($DR=D/D_p$)		2.0, 2.1, 2.2, 2.3
Punch	Diameter: D_p (mm)	9.5
	Shoulder radius: R_p (mm)	1.5
Die	Diameter: D_d (mm)	11.1
	Shoulder radius: R_d (mm)	1.0

Table 3. Experimental conditions in deep drawing test (Tsuji et al., 2009)

The effect of the DLC coating on the LDR of the Mg alloy sheet was also investigated, and DLC coated blanks were compared with blanks coated with the other lubricants in terms of the maximum punch load and the drawn-cup height. Moreover, it was determined whether the DLC coated blanks were suitable for plastic processing.

4. DLC coating and its fundamental properties

4.1 DLC coating

DLC is a general term of amorphous carbon or hydrocarbon, and there is no strict definition in chemical structure. Therefore, many kinds of hydrocarbon are used as starting material and many kinds of DLC have been prepared. In this research, we used a mixture of CH₄ and H₂ as a monomer gas for DLC coating. Figure 4 is a photograph of the original Mg alloy sheet and DLC coated Mg alloy sheet. DLC coating exhibited gold color.

Figure 5 shows deposition rate of DLC measured with the deposition monitor beside the bottom electrode, as shown in Figure 1, when the concentration of CH₄ in the gas mixture varied in total flow rate of 25 sccm. The deposition rate monotonously increased with CH₄ concentration, which is naturally expected because methane supplies main chain of DLC.



Fig. 4. Photograph of the original Mg alloy sheet (left) and DLC coated Mg alloy sheet (right)

However, the deposition rate is dependent on position in a reactor. In our research, from our previous study on the position of Mg alloy sheet for DLC coating in the reactor, underneath of the top powered electrode was found to be better than the bottom ground electrode in view of deposition efficiency and coating properties. Therefore, we placed the Mg samples underneath of the top electrode.

Since the thickness monitor is not placed near the top electrode, we measured the coating thickness directly with the surface profile system. Figure 6 shows the relationship between

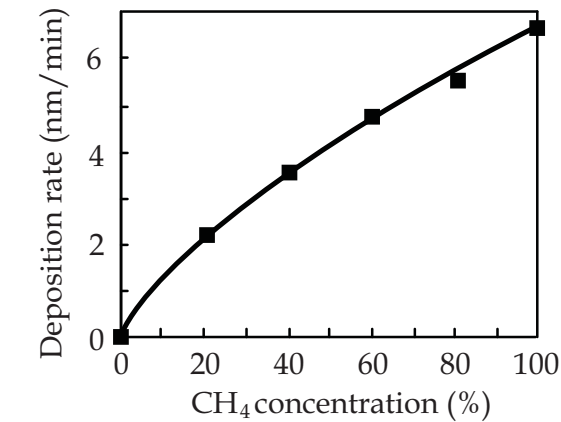


Fig. 5. Deposition rate of DLC coating as a function of CH₄ concentration in CH₄/H₂ mixture. Plasma power, 150 W; total flow rate, 25 sccm. (Iriyama et al., 2008)

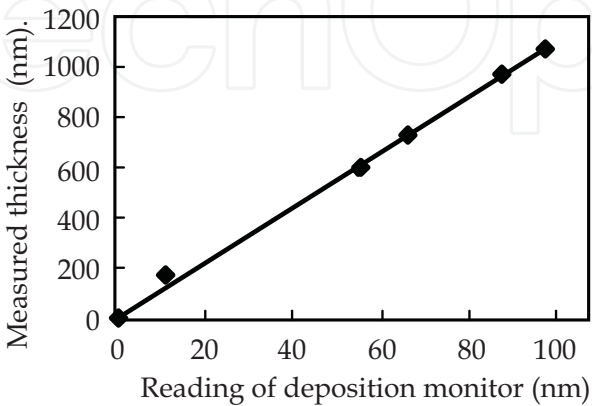


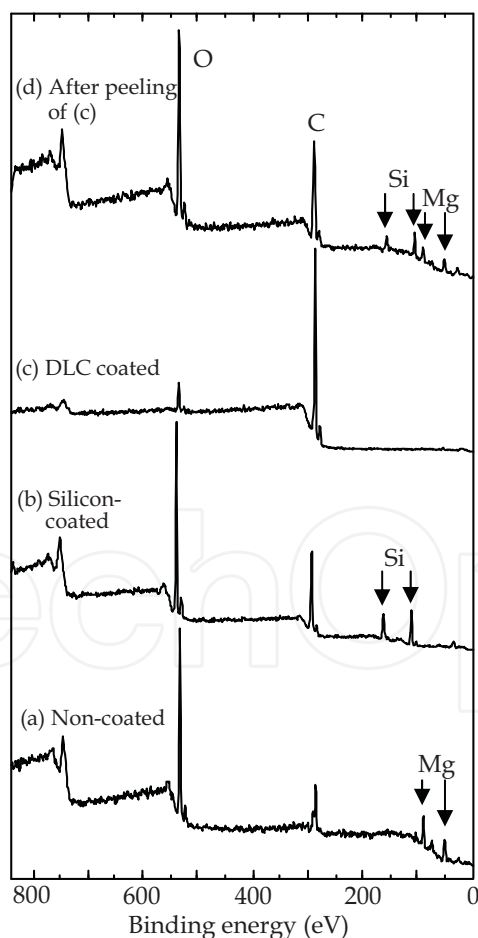
Fig. 6. Relationship of coating thicknesses between deposition-monitor readings and measured values in a surface profile system (Iriyama et al., 2008)

thicknesses measured with the deposition monitor and the surface profile measuring system. This relation is a simple proportion with the slope of 11. Therefore, we regard the actual thickness as the product of the readings of the deposition monitor multiplied by 11.

4.2 Chemical surface analysis and adhesion of DLC

In general, the adhesion between organic and inorganic materials is poor. Since DLC is categorized into an organic material, the adhesion between DLC and metal (Mg) is naturally expected to be poor. Therefore, usually, Si containing intermediate layer is inserted between them. Also in our preliminary study, most of the DLC coatings we prepared in various conditions directly on Mg alloy sheet were found to fail the peeling test. In our research, therefore, we used TEOS plasma coating for the intermediate layer. TEOS was used as a monomer and deposited on Mg alloy sheet directly before DLC coating, which is expected to improve the adhesivity.

In order to examine the chemical structure and chemical composition of the TEOS- and DLC coated Mg alloy surfaces, we analyzed them with XPS. Figure 7 shows XPS wide spectra of the surfaces of Mg alloy sheet: (a) non-coated, (b) silicon-layer coated, (c) silicon-layer and DLC coated, (d) after peeling test of (c), in which the DLC coating was intentionally removed.



(a) Non-coated; (b) silicon-layer coated; (c) silicon layer and DLC coated; (d) after surface peeling of (c). Silicon layer: 150 W, 3 min. DLC: CH₄ 60%, 150 W, 10 min.

Fig. 7. XPS wide spectra of Mg alloy sheet surfaces. (Iriyama et al., 2008)

There are naturally Mg 2s and 2p peaks at 50-100 eV on the original Mg alloy sheet. After silicon-layer coating, Mg peaks disappeared and Si 2s and 2p peaks appeared instead at 110-160 eV. After successive DLC coating, C1s peak (280-290 eV) with great intensity was found while Si signals were disappeared. Then, when the DLC coating was peeled off, C1s peak was drastically reduced and Si and Mg peaks were recovered. Since the intensity of Si and Mg signals in Fig.7d are not very strong, it is difficult to identify which interface or layer is responsible for the failure, Mg/silicon or silicon/DLC.

One of the reasons we expect the adhesivity improvement is a formation of Si-C covalent bond (Capote et al., 2008). Figure 8 shows Si2p XPS spectra of (a) TEOS coated and (b) TEOS and DLC coated Mg alloy sheet surfaces. In this particular sample for XPS, DLC was coated for only 5 nm in order for the interface to be analyzed. In TEOS coated surface (a), only Si-O peak was found, while in DLC coated surface on TEOS coating (b), Si-C peak was newly found, which is effective in the adhesivity.

Most of the cases, the adhesion is improved by the Si containing intermediate layer. But based on all the XPS results presented above, if the coating is to be peeled off, we suppose the locus of failure is the cohesive failure of silicon layer. Since silicon layer has a brittle nature, the coating conditions should be carefully selected.

In XPS analysis, deconvolution of narrow spectra could provide precise chemical structure of surfaces. Even for a hydrocarbon peak, the deconvolution enables us to distinguish sp^3 and sp^2 carbons, in which the peaks for sp^3 and sp^2 are located at around 285.2 and 284.3 eV, respectively (Mizokawa et al., 1987; J. Diaz et al., 1996). Figure 9 is an example of

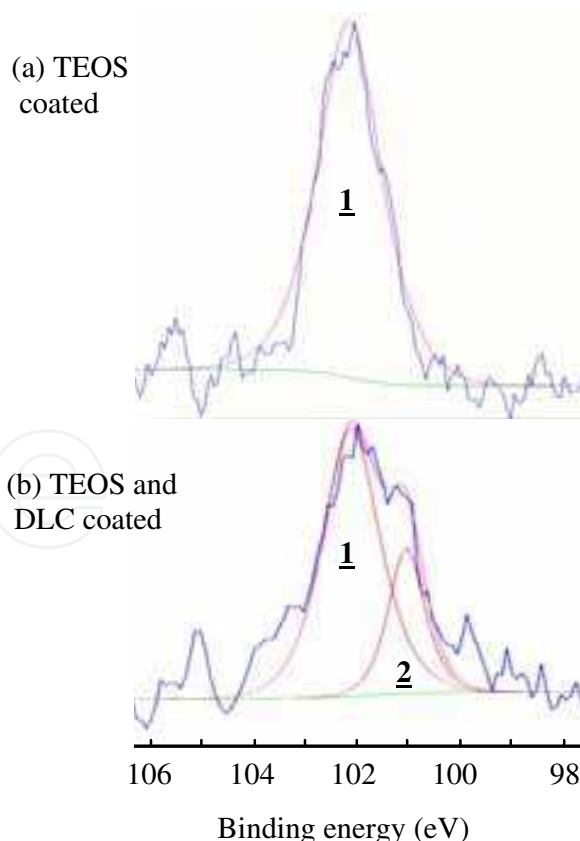


Fig. 8. Si2p XPS spectra of (a) TEOS coated and (b) TEOS and DLC coated Mg alloy sheet surfaces. 1, Si-O bond; 2, Si-C bond. (b) DLC: CH₄ 60%, ca. 5-nm thick. (Iriyama et al., 2009)

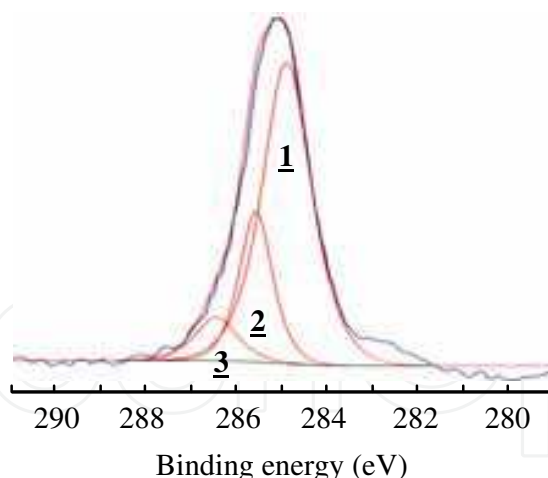


Fig. 9. C1s XPS spectrum of TEOS and DLC coated Mg alloy sheet surface. **1**, sp^2 ; **2**, sp^3 ; **3**, C-O. DLC, CH_4 60%. (Iriyama et al., 2009)

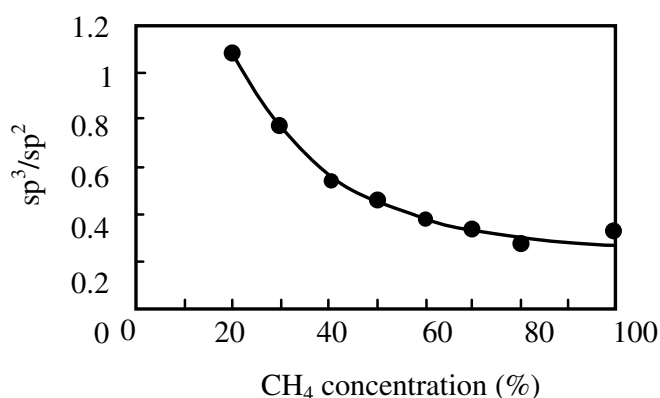


Fig. 10. Ratio of sp^3/sp^2 on the surface of DLC coated Mg alloy sheet estimated by deconvoluted C1s XPS spectra as a function of CH_4 concentration in DLC coating. (Iriyama et al., 2009)

deconvoluted C1s XPS spectrum of DLC coating. **1** and **2** in the figure represent sp^2 and sp^3 , respectively. The relationship between sp^3/sp^2 and CH_4 concentration in DLC coating is shown in Figure 10. As is expected, sp^3 decreases as the CH_4 concentration increases.

When we deal with organic materials, we are always reminded of the defect of XPS: hydrogen cannot be detected. Along with XPS, ATR-FTIR is often used for the analysis of surface chemical structure, but glow discharge spectrometry (GDS) may be the easiest technique to compensate XPS analysis. In GDS measurement, by subjecting a sample to plasma, relative contents of all the elements including H that constitute the surface of the sample are obtained by the analysis of emission in plasma. Figure 11 shows the relationship between H content and CH_4 concentration in DLC coating. The results can be naturally explained that the relative content of H found in the DLC coating was inversely proportional to CH_4 concentration in plasma gas.

Most of the cases, the silicon layer improved the adhesion of DLC on Mg alloy sheet. We measured the adhesivity of TEOS and DLC coatings deposited at various conditions on Mg alloy sheets by cross-cut test. Figure 12 shows the results of the cross-cut test for the samples coated with various TEOS flow rates (1 to 4.5 sccm) and various CH_4 concentrations (10% to 80%) in the total flow rate of 25 sccm with H_2 . The greater number of unpeeled square

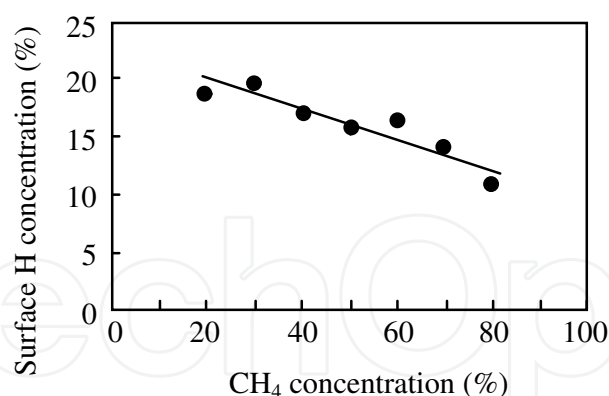


Fig. 11. Surface H concentration on DLC coated Mg alloy sheet measured by GDS as a function of CH₄ concentration in DLC coating. (Iriyama et al., 2009)

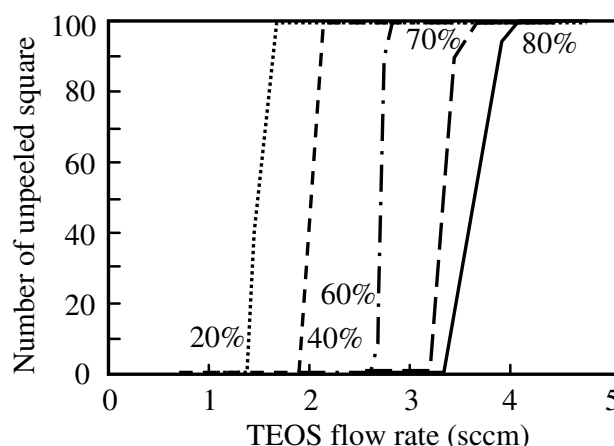


Fig. 12. The number of unpeeled squares in the adhesion test of TEOS- and DLC coated Mg alloy sheet. Percentages in the figure denote CH₄ concentration in DLC coating. (Iriyama et al., 2009)

shows greater adhesivity. As far as the deposition rate is concerned, which is dependent on the monomer concentration, higher TEOS flow rate and higher fraction of CH₄ shows greater values. Therefore, since the other plasma parameters are fixed, the thicknesses of the layers for the tested samples were varied.

From this figure, for any given CH₄ concentration, the higher TEOS flow rates show better adhesivity. Regarding the CH₄ concentration, it is interesting that the lower concentration showed better adhesivity although the coating layer is thinner. Probably, at a low deposition rate, DLC coating with good interaction with silicon layer was obtained.

Through the cross-cut test, the relatively high adhesion was found to be obtained under following conditions: TEOS, 150 W, 3-5 sccm, 1-3 min; CH₄/H₂, 150 W, 25 sccm (CH₄ 60-80%), 10 min. The thicknesses of silicon layer and DLC coating prepared under those conditions were estimated to be 50-200 and 400-600 nm, respectively.

4.3 Surface morphology and surface roughness of DLC coated Mg alloy sheet

The surface morphology of DLC coated Mg alloy sheets was observed with SEM. Figure 13 shows SEM photographs of the surfaces of Mg alloy sheet coated by different manner. When

DLC was coated directly on Mg (Fig.13b), oriented long flakes are found, which are obviously ready to come out. When only TEOS was coated on Mg (Fig.13c), on the other hand, a regular dense waving pattern was found, which looked tight and rigid and seems to have good adhesion and might be favorable in lowering the surface friction coefficient. This pattern was found on the most of TEOS coated Mg alloy sheets but not on the direct DLC coating on Mg regardless of the CH_4 concentration. The adhesivity could be judged by the close look of those photographs. Then, when DLC was coated after TEOS coating (Fig.13d), the appearance did not change from TEOS coating (Fig.13c), keeping the waving pattern, and the adhesivity seems to be good. When DLC was coated thicker (30 min) after TEOS coating (Fig.13e), a high internal stress caused peeling, but it is interesting to refer that the waving pattern of TEOS coating has been inherited.

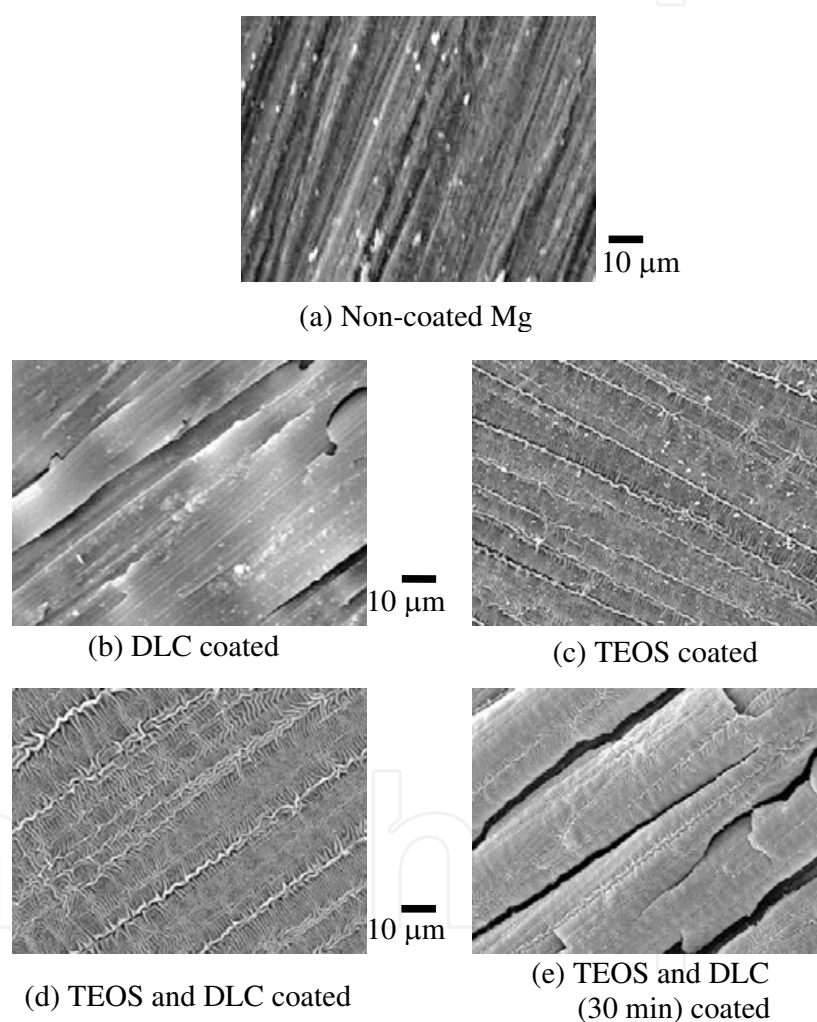


Fig. 13. SEM photographs of (a) non-coated, (b) TEOS coated, (c) DLC coated, and (d, e) Si and DLC coated Mg alloy sheet surfaces. (d, e) DLC, CH_4 60%; (e) DLC, 30 min. (Iriyama et al., 2009)

Figure 14 shows the surface roughness curves of the non-coated and DLC coated Mg alloy sheets. As shown in the figure, R_z and R_a for non-coated Mg alloy sheet were 1.65 and 0.24 μm , respectively, while those of DLC coated Mg alloy sheet were 1.78 and 0.21 μm , respectively. Those values were comparable, and it is confirmed that the surface roughness remains almost unchanged by DLC coating.

4.4 Surface friction of DLC coated Mg alloy sheet

Figure 15 shows approximate friction coefficient-sliding distance curves of various Mg alloy sheets. They are, three DLC coated (different plasma condition) and two lubricant-coated (MoS₂ and GM100) Mg alloy sheets along with non-coated one. The average friction coefficient for each specimen calculated based on this figure is shown in Table 4. It is possible to reduce the surface friction coefficient of DLC to less than 0.1 if you want to, but our objective was to obtain the friction coefficient comparable to MoS₂. The friction coefficient of DLC coated Mg alloy sheet was reduced significantly from 0.42 to 0.16-0.18, which is the same level to MoS₂ lubricated one. For a DLC coating in general, the friction coefficient of 0.16-0.17 is not very low, but it is low enough for the present application, and other factors may be contributed to the formability of the Mg alloy sheet.

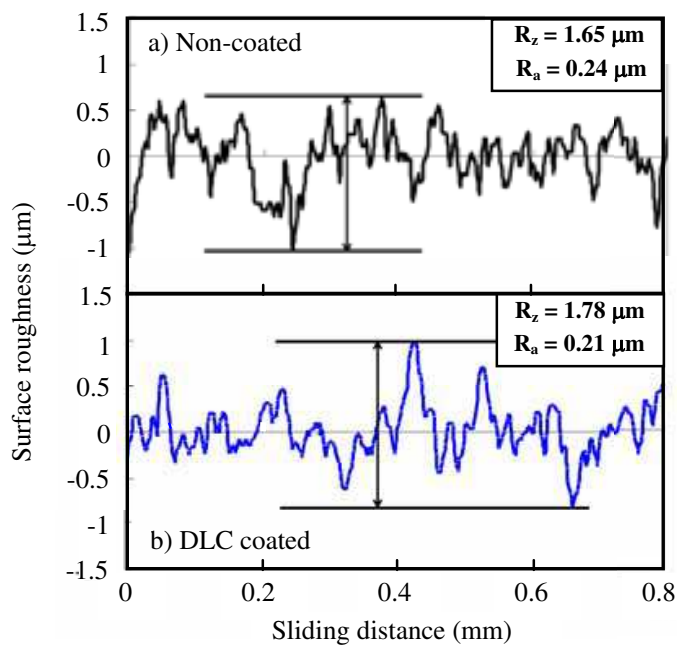


Fig. 14. Surface roughness curves of (a) non-coated and (b) DLC coated Mg alloy sheets (Tsuji et al., 2009)

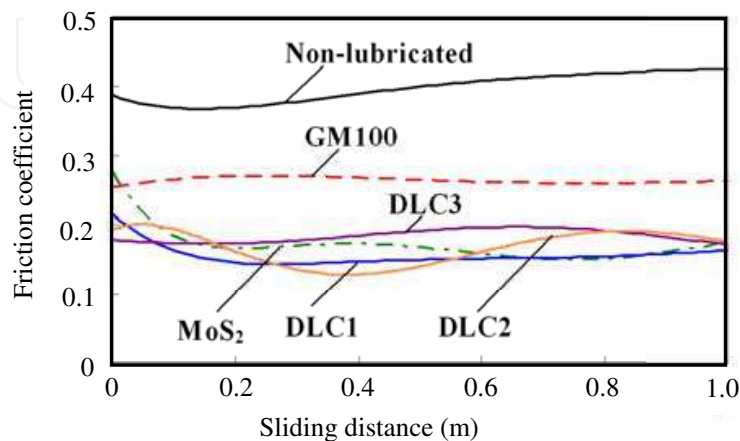


Fig. 15. Friction coefficient of DLC- and lubricant-coated Mg alloy sheets (Tsuji et al., 2009)

Type of lubricant	Friction coefficient
DLC1	0.16
DLC2	0.17
DLC3	0.18
MoS ₂	0.17
GM100	0.26
Non-lubricated	0.42

Table 4. Friction coefficient of DLC- and lubricant-coated Mg alloy sheets (Tsuji et al., 2009)

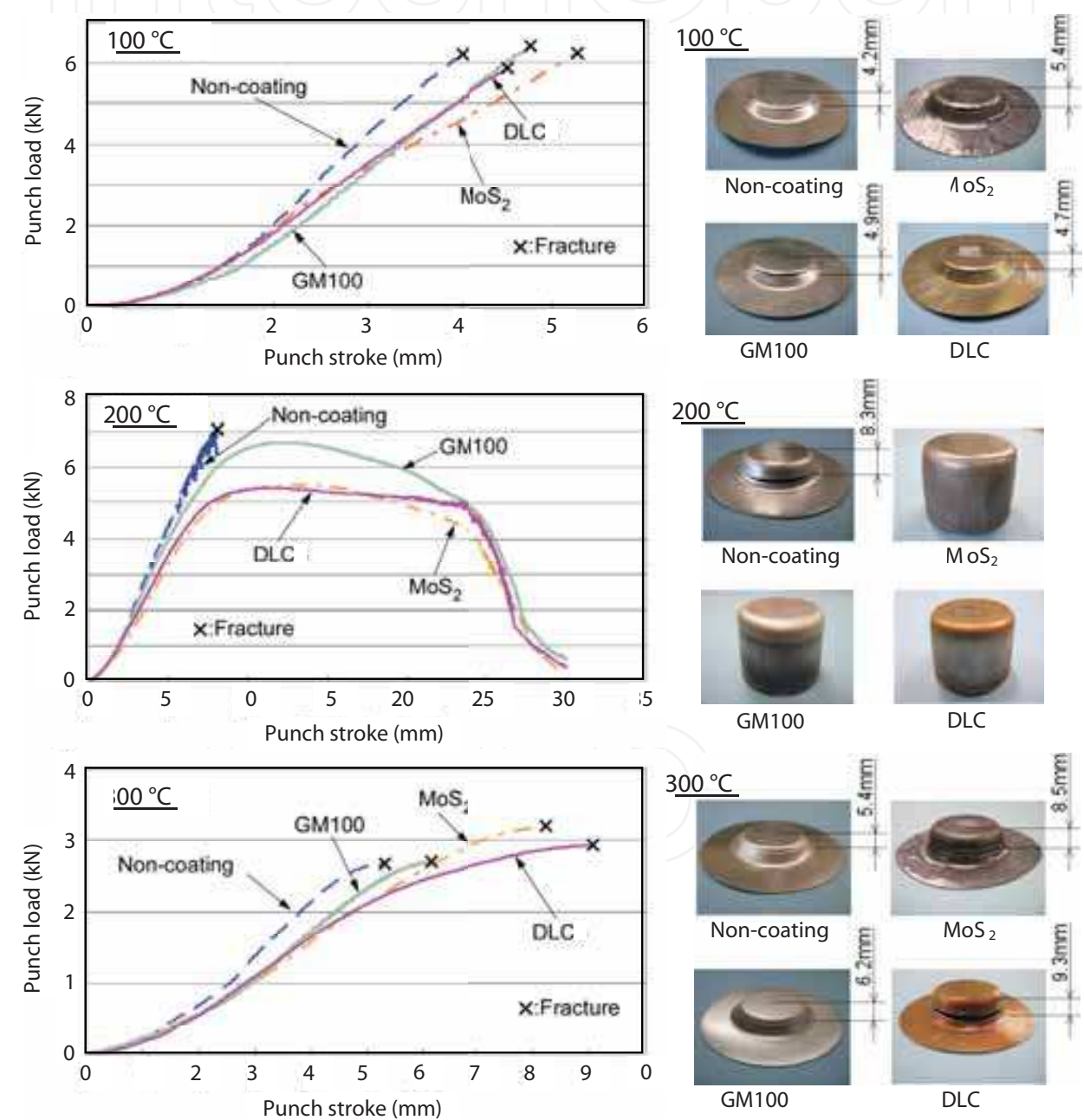


Fig. 16. Punch load-punch stroke curves for DLC- and lubricant-coated Mg alloy sheets at various temperatures, and photographs of the drawn cups. (Tsuda et al., 2008)

4.5 Circular-cup deep-drawing test

The ultimate objective of this research “better formability” comes to press forming and deep drawing. For the circular-cup deep-drawing test, we used DLC coatings with small friction coefficient because there is a clear correlation between friction coefficient and formability. Figure 16 depicts punch load-punch stroke curves and the photographs of the drawn cup at 100, 200 and 300 °C for DLC and other lubricant-coated Mg alloy sheets. Table 5 shows the maximum punch load and punch stroke at the maximum punch load point under various conditions and temperatures.

At 100 °C, the height of the drawn cup of DLC coating was the same as the height of the drawn cup of MoS₂ and GM100. These results were superior to those obtained in the case of non-coating at the maximum punch load and punch stroke. At this temperature, little effect of lubrication including DLC coating observed: difference of deep drawability among the lubricated Mg alloy sheets was not ascertained.

At 200 °C, in case of DLC coating, MoS₂, and GM100, samples survived the complete deep-drawing process without fracture. Moreover, the maximum punch load of the DLC coating and MoS₂ was 5.39 and 5.47 kN, respectively: 5.39 kN for DLC coated Mg alloy sheet was the lowest in any other conditions. Non-coated one immediately fractured. DLC coated Mg alloy sheet had good deep drawability comparable to that for MoS₂ lubricated one.

At 300 °C, in case of DLC coating the punch stroke was the longest of any other conditions. It was observed that the DLC coating reduces the punch load and affects deep drawability. It was confirmed that the DLC coating has a distinct lubrication capability which is as good as the lubricant for the plastic processing of a Mg alloy sheet. Furthermore, it was made clear that DLC coating improves the deep drawability of Mg alloy sheet.

Conditions of lubricant	Max. punch load (kN)			Punch stroke (mm) (Max. punch load point)		
	100 °C	200 °C	300 °C	100 °C	200 °C	300 °C
DLC coating	5.84	5.39	2.94	4.53	11.44	9.08
MoS ₂	6.21	5.47	3.20	5.27	13.10	8.35
GM100	6.39	6.72	2.70	4.78	12.16	6.71
Non coating	6.21	7.14	2.67	4.03	8.12	5.32

Table 5. Maximum punch load and punch stroke (Tsuda et al., 2008)

Figure 17 is the success-fail diagram of circular-cup deep-drawing for DLC coated and GM100 lubricated Mg alloy sheets. In this figure, circle mark “O” indicates successful of deep-drawing, “X” the fracture at the punch shoulder, and triangle mark the fracture at the wall.

The LDRs for the deep-drawing of DLC coated and GM100 lubricated Mg alloy sheets were predicted from the intersection of the two thick lines in the figure. For the determination of the LDR, deep-drawing tests were carried out under conditions similar to those at the intersection. As results, Mg alloy sheet was possible to deform up to LDR= 2.23 for DLC coated and LDR= 2.20 for GM100 lubricated.

In general, the LDR for circular-cup deep-drawing is obtained from fracture of the punch shoulder. However, in these tests, the fracture occurred at the side wall section area where the surface was subjected to reasonably tensile stress generation because the die shoulder was heated.

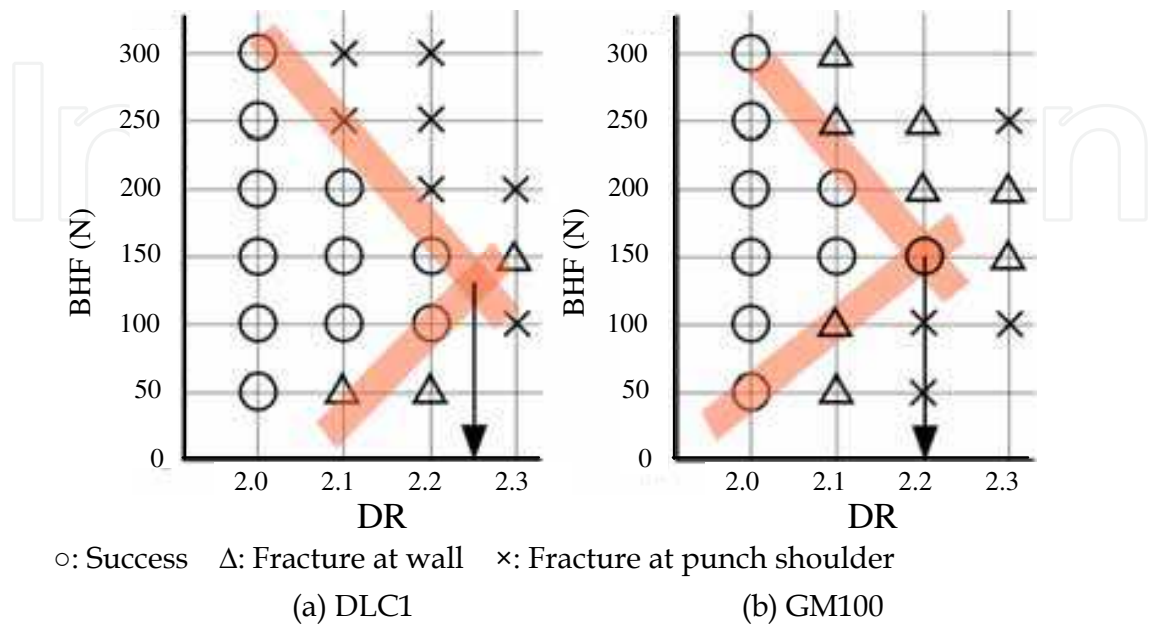


Fig. 17. Limiting drawing ratio (LDR) of (a) DLC coated and (b) GM100 lubricated Mg alloy sheets (Tsuji et al., 2009)

Table 6 shows the circular-cup deep-drawability with the blank holder force of 150 N at 200 °C. As explained in Fig.18, the LDR for DLC and GM100 was 2.23 and 2.20. On the other hand, the LDR for MoS₂ lubricated Mg alloy sheet was 2.3 and that for non-coated one was 1.9. Although the surface friction coefficient of DLC coated and MoS₂ lubricated Mg alloy sheet was comparable level in the friction test, the LDR was difference between DLC and MoS₂. It is considered that DLC film was exfoliated due to effect on the frictional resistance at the die shoulder part, and the frictional force was increased by exfoliation of the DLC film.

Type \ DR	DR					
	1.9	2.0	2.1	2.2	2.3	2.4
DLC coated	-	○	○	LDR2.23		-
MoS ₂	-	○	○	○	○	×
GM100	-	○	○	LDR2.20		-
Non-lubricated	○	×	-	-	-	-

○: Success ×: Fracture -: Untested

Table 6. Deep drawability under several friction conditions (BHF: 150 N, T: 200 °C) (Tsuji et al., 2009)

Figure 18 shows the distribution of the wall thickness from the bottom to the edge of the drawn-cup with a DLC coated in the directions of RD- and TD-cross-sections. The wall thickness was the same as the initial thickness at the bottom of the drawn-cup. The reduction of the wall thickness and tensile elongation at the punch shoulder were confirmed in both directions and the thickness increased at the side wall. On the other hand, the reduction in thickness of the punch shoulder and the deformation in the RD-cross-section direction were inhibited in comparison with that in the TD-cross-section direction. The reason was the effect of the anisotropy (r value) of the Mg alloy sheet. For the evaluation of the lubricating performance of the DLC coating, three wall thickness distribution points at the punch shoulder, at the side wall part, and at the brim of the cup were compared with those for GM100 lubricated Mg alloy sheets. The reduction of the wall thickness for DLC coated was less than that for GM100 lubricated. As a result, it was confirmed that the DLC coating has good lubricating performance compared with GM100.

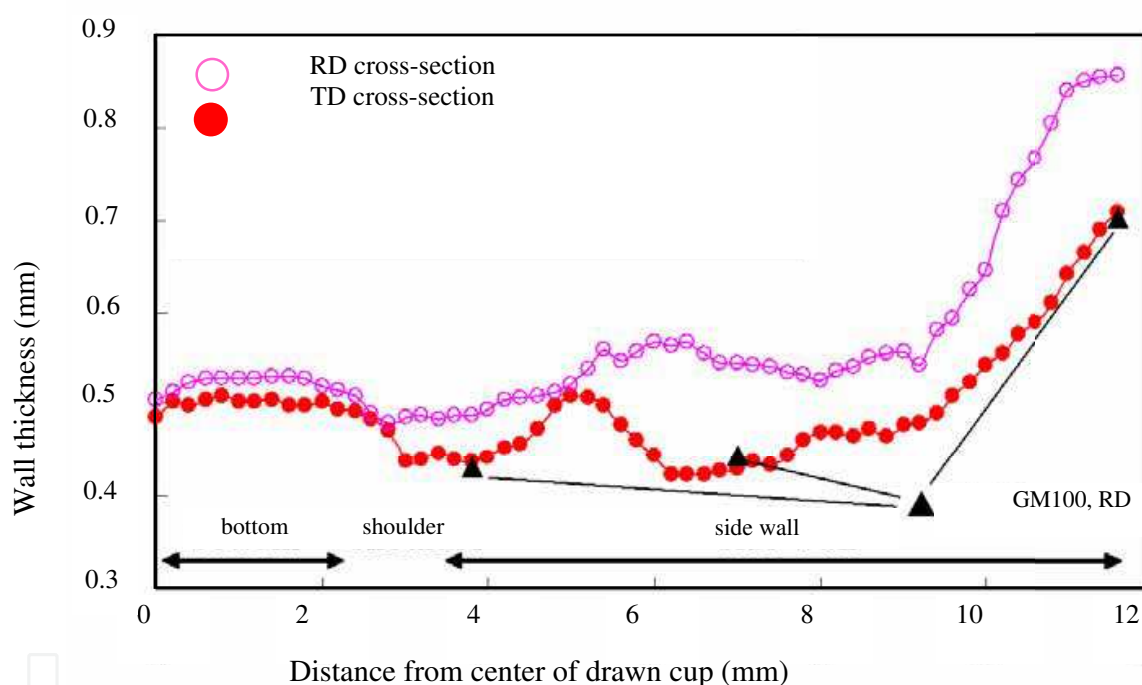


Fig. 18. Wall thickness distribution of drawn cup of DLC coated Mg alloy sheet. BHF, 150 N; temperature, 200 °C; DR, 2.1. (Tsuji et al., 2009)

5. DLC Coating on aluminum alloy sheet

As a comparison to Mg alloy sheet, DLC was coated on aluminium (Al) alloy sheet, another versatile light metal. Also in the press forming of Al alloys, lubricating oil is used to prevent the adhesion of Al alloys to the forming tools. Therefore, new lubricating techniques, preferably dry system, are an urgent necessity.

Al alloy sheet used in this experiment was A5052-O (0.5-mm thick). Disk of the Al alloy sheet (18.05-mm d.) was used for both friction test and deep drawing.

DLC was coated in the same manner as that on Mg alloy sheet. Also, the conventional lubricant GM100 was used for a comparison.

Figure 19 shows the results of peeling test, which depicts the adhesivity of DLC on Al alloy sheet. If you compare this figure with Fig.12, which corresponds to Mg alloy sheet, you will see that Al has less dependency on TEOS flow rate: Al alloy sheet can achieve good adhesivity at wide plasma deposition condition.

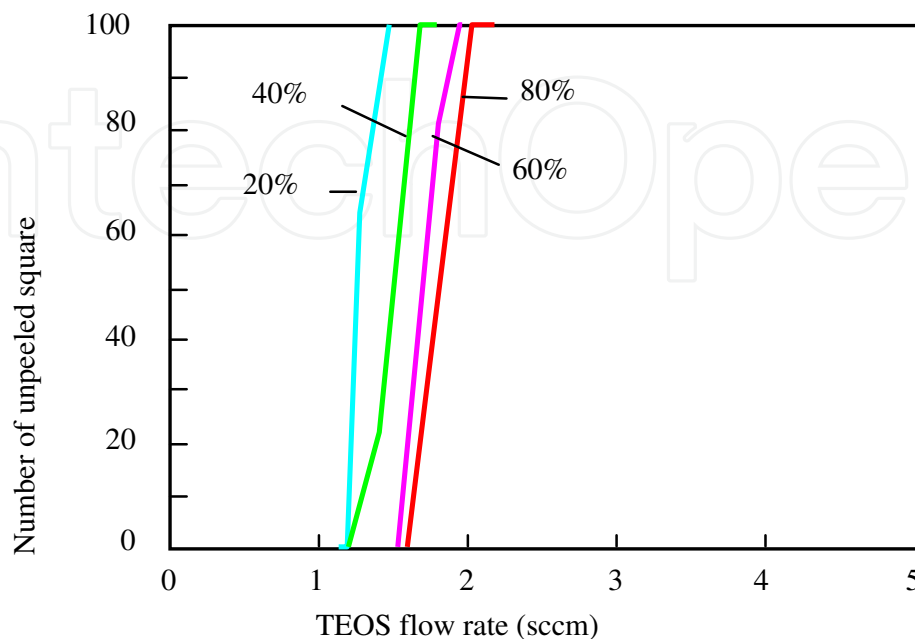


Fig. 19. The number of unpeeled squares in the adhesion test of TEOS- and DLC-coated Al alloy sheet. Percentages in the figure denote CH₄ concentration in DLC coating.

Figure 20 shows approximate friction coefficient-sliding distance curves at (a) room temperature and (b) 200 °C.

At room temperature, the average friction coefficient of non-coated Al alloy sheet was 0.60, which was reduced to 0.43 by GM100 lubrication. Further, much lower values, 0.16-0.2, were marked by DLC coated ones, which exhibited good lubricating performance.

At 200 °C, extremely low friction coefficient, 0.03, was obtained by two of three DLC coated ones, while that of GM100 lubricated one was reduced somewhat. On the contrary, that of non-coated one was increased, because the adhesivity of the aluminum alloy increased with temperature. From these results, DLC coating is expected to have a good property for deep drawing, too.

Figure 21 shows the punch load curves in deep drawing of (a) DLC coated and (b) GM100 lubricated Al alloy sheets at 200 °C. The deep-drawing apparatus used for Al alloy sheet was a compact press-forming machine, which is different from the one used for Mg alloy sheet. The deep-drawing test was conducted at a punch thrust force of 5 kN and three punch speeds, 0.05, 0.5, and 5.0mm/s, for the investigation of the effect of the strain ratio on deep-drawability.

From this figure, it was found that the maximum punch load of DLC coated Al alloy sheet was about 40% less than that of GM100 lubricated one at each punch speed. The deep-drawing of DLC coated Al alloy sheet was also completed at room temperature, but the maximum punch load exceeded 2 kN for all punch speeds.

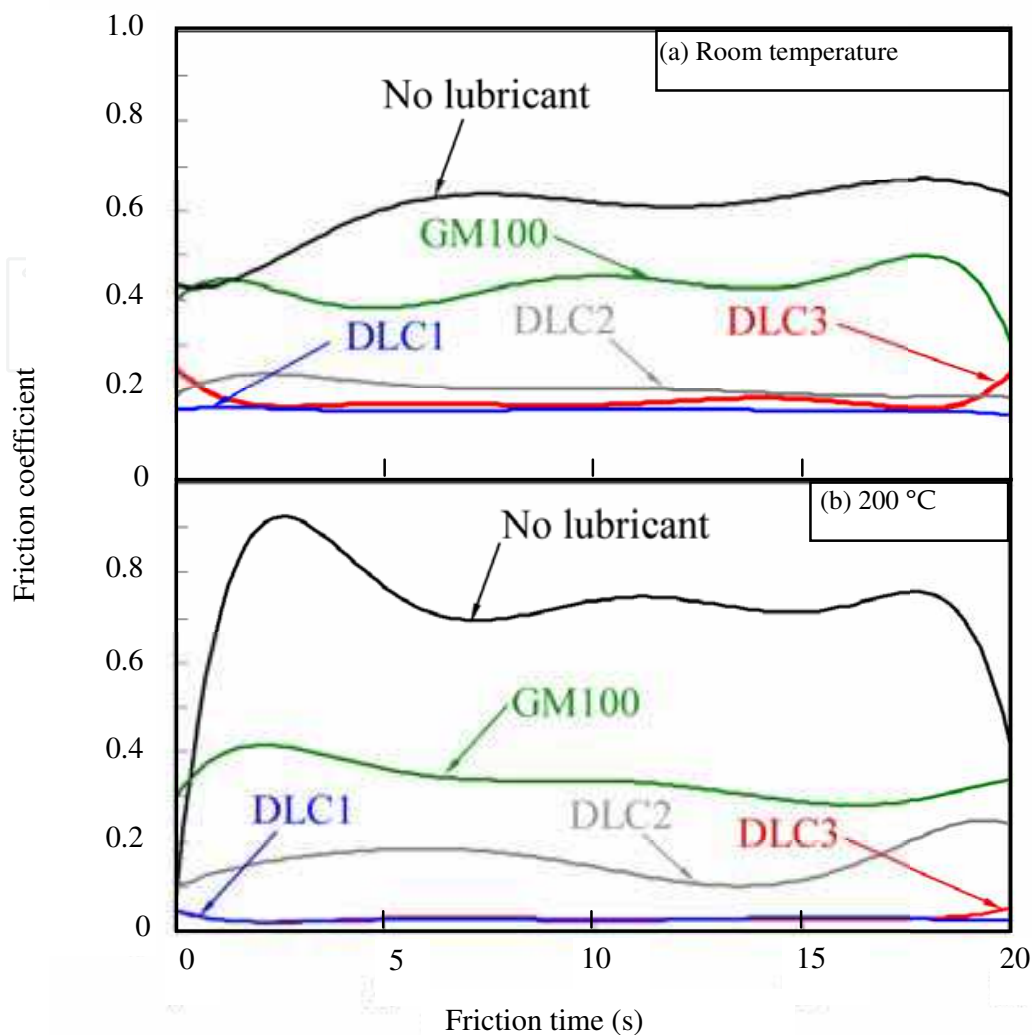


Fig. 20. Friction coefficient-friction time curves of DLC coated and GM100 lubricated Al alloy sheets at (a) room temperature and (b) 200 °C (Horiuchi et al., 2010)

As for the relationship between the punch load and the maximum punch speed, there is a regular correlation as shown in Fig. 21: the punch load increased with the punch speed. On the contrary, in the deep-drawing of DLC coated Al alloy sheet at room temperature, an inverse correlation was found: the punch load decreased with increasing punch speed. These phenomena can be explained by the strain rate sensitivity (m value) of A5052. The m value is positive at 200 °C, but it is negative at room temperature. From these results, the maximum punch load is affected by the dependence of the punch speed on temperature.

6. Conclusion

DLC coating on Mg alloy sheet had a good adhesion by the support of the intermediate silicon layer, which have not increased or induced exfoliation. DLC coating on Mg alloy sheet, which had a high lubricating capability, reduced the surface friction coefficient to the same level for MoS₂ lubricant. The deep-drawing of DLC coated Mg alloy sheet was successful at 200 °C. It was confirmed that the LDR of DLC coated Mg alloy sheet was 2.23,

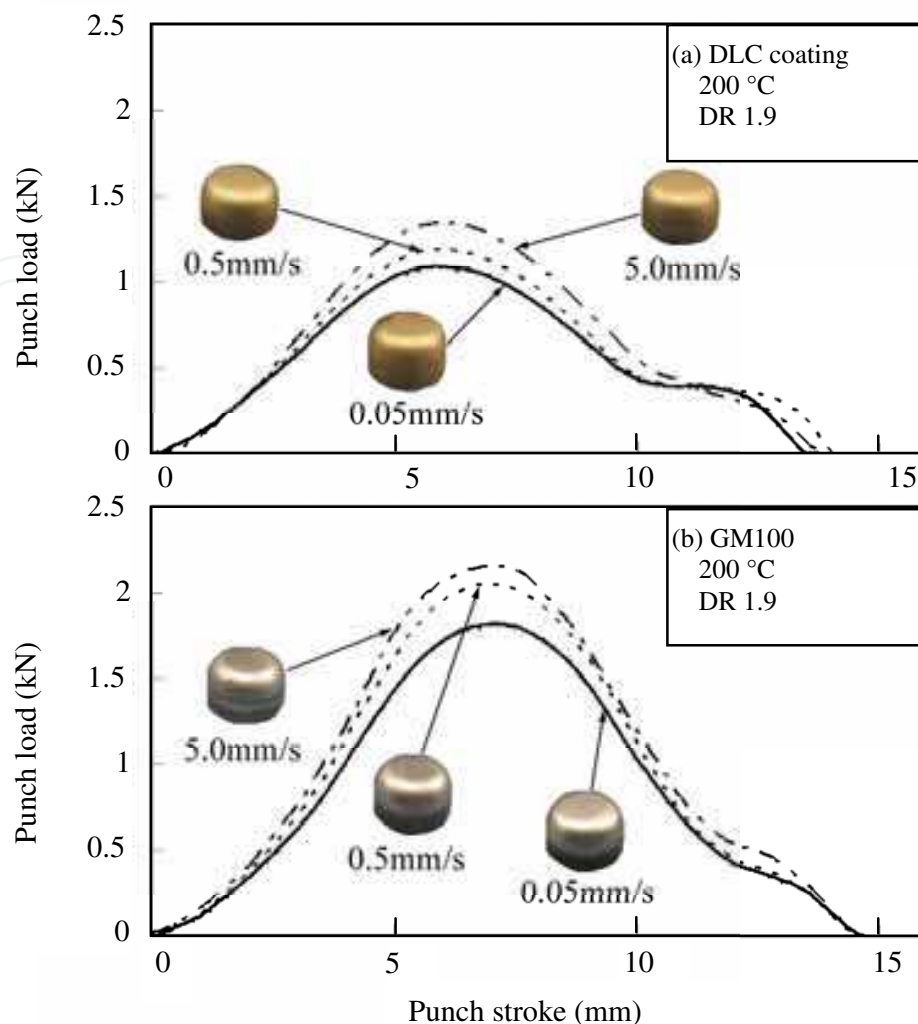


Fig. 21. Punch load-punch stroke curves for (a) DLC coated and GM100 lubricated Al alloy sheets at varied punch speeds. (Horiuchi et al., 2010)

while those of MoS₂ and GM100 lubricated Mg alloy sheet were 2.30 and 2.20, respectively. The punch load of DLC coated Mg alloy sheet was lower than those of MoS₂ and GM100 lubricated ones. It is concluded that the use of the DLC coating improved the formability of Mg alloy sheet compared with the use of other lubricants. Similar results were also found on the DLC coated Al alloy sheet. The formability will be further improved by the optimization of DLC coating conditions.

This technique, coating on forming material rather than die, is useful for complex-shaped press forming. It is necessary for DLC coating to have a good adhesivity for better formability, but one of the ultimate goals is self-removal after press forming.

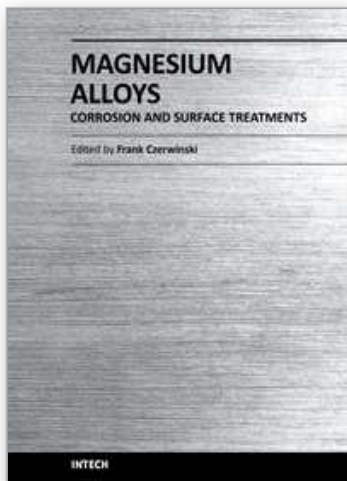
7. References

Capote, G.; Bonetti, L. F.; Santos, L. V.; Trava-Airoldi, V. J. & Corat, E. J. (2008). Adherent amorphous hydrogenated carbon films on metals deposited by plasma enhanced chemical vapor deposition. *Thin Solid Films*, 516(12), 4011-4017.

- Choi, J.; Nakao, S.; Kim, J.; Ikeyama, M. & Kato, T. (2007a). Corrosion protection of DLC coatings on magnesium alloy. *Diamond Relat. Mater.*, 16(4-7), 1361-1364.
- Choi, J.; Kim, J.; Nakao, S.; Ikeyama, M. & Kato, T. (2007b). Friction properties of protective DLC films on magnesium alloy in aqueous NaCl solution. *Nucl. Instrum. Methods Phys. Res., Sect. B*, 257(1-2), 718-721.
- D'Errico, G. E.; Calzavarini, R. & Vicenzi, B. (1998). Influence of PVD coatings on cermet tool life in continuous and interrupted turning. *J Mater. Proc. Technol.*, 78, 53-58.
- Diaz, J.; Paolicelli, G.; Ferrer, S. & Comin, F. (1996). Separation of the sp^3 and sp^2 components in the C1s photoemission spectra of amorphous carbon films. *Phys. Rev.*, B54(11), 8064-8069.
- Dai, W.; Wu, G. & Wang, A. (2010). Preparation, characterization and properties of Cr-incorporated DLC films on magnesium alloy, *Diamond Rel. Mater.*, 19(10), 1307-1315.
- Horiuchi, T.; Yoshihara, S. & Iriyama, Y. (2010). Deep drawability of DLC-coated A5052 Aluminum alloy sheet. *Proceedings of 4th International Conference on Tribology in Manufacturing Processes - ICTMP 2010*, pp.691-700, Nice, France, June 2010.
- Iriyama, Y.; Sakurai, S.; Yoshihara, S. & Tsuda, S. (2008). "Reduction of friction coefficient of magnesium alloy sheet by DLC coating with low-temperature plasma. *J Photopolym. Sci. Technol.*, 21(2), 245-250.
- Iriyama, Y.; Nakano, Y.; Yoshihara, S. & Tsuji, Y. (2009). DLC coating on magnesium alloy sheet by low-temperature plasma" *J Photopolym. Sci. Technol.*, 22(4), 485-490.
- Kataoka, S.; Murakawa, M.; Aizawa, T. & Ike, H. (2004). Tribology of dry deep-drawing of various metal sheets ceramics tools. *Surf. Coat. Technol.*, 177-178, 582-590.
- Kataoka, S.; Motoi, A.; Tamaoki, K.; Murakawa, M.; Noguchi, H. & Kihara, J. (2005). Improvement in DLC thin film adhesion and its application to dry deep drawing. *J Jpn. Soc. Technol. Plast.*, 46(532), 412-416 (in Japanese).
- Kataoka, S. (2006). Tools for dry press working, *J Jpn. Soc. Technol. Plast.*, 47(546), 569-573 (in Japanese).
- Konca, E.; Cheng, Y.-T. & Alpas, A. T. (2006). Sliding wear of non-hydrogenated diamond-like carbon coatings against magnesium. *Surf. Coat. Technol.*, 201(7), 4352-4356.
- Mizokawa, Y.; Miyasato, T.; Nakamura, S.; Geib, M. & Wilmsen, C. W. (1987). The C *KLL* first-derivative x-ray photoelectron spectroscopy spectra as a fingerprint of the carbon state and the characterization of diamondlike carbon films. *J Vac. Sci. Technol.*, A5(5), 2809-2813.
- Reisal, G.; Wielage, B.; Steinhauser, S. & Hartwig, H. (2003). DLC for tools protection in warm massive forming. *Diamond Rel. Mater.*, 12, 1024-1029.
- Tamaoki, K.; Kataoka, S. & Minamoto, K. (2006). Dry cylindrical cup drawing using electroconductive ceramic tools. *J Jpn. Soc. Technol. Plast.*, 48, 930-934 (in Japanese).
- Tamaoki, K.; Kataoka, S.; Kanda, K. & Takano, S. (2007). Applying CVD diamond film to alloy tool steels. *Proceedings of the 2007 Japanese Spring Conference for the Technology of Plasticity*, p.177 (in Japanese).
- Tillmann, W.; Vogli, E.; Gathen, M. & Momeni, S. (2009). Development of wear resistant pressing moulds for the production of diamond composites. *J Mater. Proc. Technol.*, 209, 4268-4273.
- Tsuda, S.; Yoshihara, S.; Tsuda, S.; Iriyama, Y. & Sakurai, S. (2008). Effect of DLC coating on deep drawability of AZ31 magnesium alloy sheet. *Proceedings of the 25th*

- International Manufacturing Conference, IMC 25*, pp.23-30, Dublin Institute of Technology, Ireland, Sep. 2008.
- Tsuji, Y.; Yoshihara, S.; Tsuda, S.; Iriyama, Y. & Nakano, Y. (2009). Effect of DLC coating on limiting drawing ratio of AZ31 magnesium alloy sheet. *Proceedings of the ASME 2009, International Mechanical Engineering Congress & Exposition, IMECE2009-10947*, pp.1-6, Lake Buena Vista, Florida, USA, Nov. 2009.
- Yamauchi, N.; Demizu, K.; Ueda, N.; Cuong, N. K.; Sone, T. & Hirose, Y. (2005). Friction and wear of DLC films on magnesium alloy. *Surf. Coat. Technol.*, 193(1-3), 277-282.
- Yamauchi, N.; Ueda, N.; Okamoto, A.; Sone, T.; Tsujikawa, M. & Oki, S. (2007). DLC coating on Mg-Li alloy. *Surf. Coat. Technol.*, 201(9-11), 4913-4918.
- Yoshihara, S.; Yamamoto, H.; Manabe, K. & Nishimura, H. (2003). Formability Enhancement in magnesium alloy deep drawing by local heating and cooling technique. *J Mater. Proc. Technol.*, 143-144, 612-615.
- Yoshihara, S.; Manabe, K. & Nishimura, H. (2005). Effect of blank holder force control in deep-drawing process of magnesium alloy sheet. *J Mater. Proc. Technol.*, 170, 579-585.
- Wu, G.; Sun, L.; Dai, W.; Song, L. & Wang, A. (2010). Influence of interlayers on corrosion resistance of diamond-like carbon coating on magnesium alloy, *Surf. Coat. Technol.*, 204(14), 2193-2196.

IntechOpen



Magnesium Alloys - Corrosion and Surface Treatments

Edited by Frank Czerwinski

ISBN 978-953-307-972-1

Hard cover, 344 pages

Publisher InTech

Published online 14, January, 2011

Published in print edition January, 2011

A resistance of magnesium alloys to surface degradation is paramount for their applications in automotive, aerospace, consumer electronics and general-purpose markets. An emphasis of this book is on oxidation, corrosion and surface modifications, designed to enhance the alloy surface stability. It covers a nature of oxides grown at elevated temperatures and oxidation characteristics of selected alloys along with elements of general and electrochemical corrosion. Medical applications are considered that explore bio-compatibility of magnesium alloys. Also techniques of surface modifications, designed to improve not only corrosion resistance but also corrosion fatigue, wear and other behaviors, are described. The book represents a valuable resource for scientists and engineers from academia and industry.

How to reference

In order to correctly reference this scholarly work, feel free to copy and paste the following:

Yu Iriyama and Shoichiro Yoshihara (2011). DLC Coating on Magnesium Alloy Sheet by Low-Temperature Plasma for Better Formability, Magnesium Alloys - Corrosion and Surface Treatments, Frank Czerwinski (Ed.), ISBN: 978-953-307-972-1, InTech, Available from: <http://www.intechopen.com/books/magnesium-alloys-corrosion-and-surface-treatments/dlc-coating-on-magnesium-alloy-sheet-by-low-temperature-plasma-for-better-formability>

INTECH
open science | open minds

InTech Europe

University Campus STeP Ri
Slavka Krautzeka 83/A
51000 Rijeka, Croatia
Phone: +385 (51) 770 447
Fax: +385 (51) 686 166
www.intechopen.com

InTech China

Unit 405, Office Block, Hotel Equatorial Shanghai
No.65, Yan An Road (West), Shanghai, 200040, China
中国上海市延安西路65号上海国际贵都大饭店办公楼405单元
Phone: +86-21-62489820
Fax: +86-21-62489821

© 2011 The Author(s). Licensee IntechOpen. This chapter is distributed under the terms of the [Creative Commons Attribution-NonCommercial-ShareAlike-3.0 License](https://creativecommons.org/licenses/by-nc-sa/3.0/), which permits use, distribution and reproduction for non-commercial purposes, provided the original is properly cited and derivative works building on this content are distributed under the same license.

IntechOpen

IntechOpen